Tutorial 13: Quark masses and mixings

Dr. M Flowerdew

June 1, 2015

1 The CKM matrix

In tutorial 3, we wrote down the SM Lagrangian for one quark/lepton generation. The emphasis was on the BEH mechanism and mass in the boson sector, however we also noted that the treatment of the fermion sector depends on the number of fermion generations. Extended to three generations, the Yukawa couplings for the quarks become 3×3 matrices Y_u^{ij} and Y_d^{ij}, where the indices i and j indicate the generation number. The quark mass terms in the Lagrangian therefore become[1]

$$\mathcal{L}_{m_q} = -\bar{q}_{\mathrm{L}}^i \phi Y_d^{ij} d_{\mathrm{R}}^j - \left(-\bar{d}_{\mathrm{L}}^i \quad \bar{u}_{\mathrm{L}}^i\right) \phi^* Y_u^{ij} u_{\mathrm{R}}^j + \mathrm{h.c.} \tag{1}$$

The matrices Y_u^{ij} and Y_d^{ij} need not be real, but must be Hermitian, and can be diagonalised via a unitary transformation:[2]

$$
\begin{aligned}
u_{\mathrm{L}}' &= U_u^\dagger u_{\mathrm{L}}, & u_{\mathrm{R}}' &= V_u^\dagger u_{\mathrm{R}}, \\
d_{\mathrm{L}}' &= U_d^\dagger d_{\mathrm{L}}, & d_{\mathrm{R}}' &= V_d^\dagger d_{\mathrm{R}}.
\end{aligned}
\tag{2}
$$

If we repeat the above exercise, giving generation indices to the gauge fields, it is easy to see that, for example, $\bar{d}_{\mathrm{L}}'^i \boldsymbol{G}_\mu^{ij} d_{\mathrm{L}}'^j = \bar{d}_{\mathrm{L}}^i \boldsymbol{G}_\mu^{ij} d_{\mathrm{L}}^j$ is left unmodified. This is true for all of the Lagrangian terms associated with the exchange of electrically neutral gauge bosons (γ, Z, g), and these interactions are therefore unaffected by the transformation of Equation (2). In the case of W boson exchange (the only SM charged current), the terms in the Lagrangian couple up-type fields to down-type fields, and therfore gain factors of either $(U_u^\dagger U_d)^{ij}$ or its Hermitian conjugate. Thus, the entire description of flavour mixing in the SM is dependent on a single 3×3 Hermitian matrix, called the *CKM* matrix after its inventors Cabibbo, Kobayashi and Maskawa:

$$V_{\mathrm{CKM}} = U_u^\dagger U_d = \begin{pmatrix} V_{ud} & V_{us} & V_{ub} \\ V_{cd} & V_{cs} & V_{cb} \\ V_{td} & V_{ts} & V_{tb} \end{pmatrix}. \tag{3}$$

---

[1] The quark fields in Equation (1) refer to the *interaction basis*, where the W boson only couples quarks within a generation, not between generations.

[2] Here, and for the rest of this section, the generation indices on u_{L} etc. are implicit.

In terms of Feynman rules, the elements of V_{CKM} appear as additional factors at $q - \bar{q}' - W$ vertices, effectively modifying the weak coupling g.

The CKM matrix, as a 3×3 complex matrix, would appear to have 18 free parameters. However, the unitarity condition $V_{\text{CKM}}^{\dagger} V_{\text{CKM}} = \mathbf{1}$ imposes nine constraints (one for each element), leaving nine free parameters – three mixing angles and six complex phases. Five of these phases can be removed by further redefinitions of the quark fields (e.g. $u_{\text{L}} \to e^{i\phi_u} u_{\text{L}}$ etc.), which do not affect the gauge or Higgs interactions at all.

Exercise: Why can we not redefine the phases of all six quark fields? *Hint:* consider the transformation $V_{\text{CKM}} \to \text{diag}(e^{-i\phi_u}, e^{-i\phi_c}, e^{-i\phi_t}) \cdot V_{\text{CKM}} \cdot \text{diag}(e^{i\phi_d}, e^{i\phi_s}, e^{i\phi_b})$ and find a way to reduce the number of independent phases to five. Try again to reduce it to four – why does this not work?

Thus, only three angles and one phase are physically relevant. For our purposes, it is more enlightening to re-express these four parameters in another way, called the *Wolfenstein parameterisation*:

$$V_{\text{CKM}} = \begin{pmatrix} 1 - \frac{\lambda^2}{2} & \lambda & A\lambda^3(\rho - i\eta) \\ -\lambda & 1 - \frac{\lambda^2}{2} & A\lambda^2 \\ A\lambda^3(1 - \rho - i\eta) & -A\lambda^2 & 1 \end{pmatrix} \qquad (4)$$

This takes advantage of the observed hierarchy in the CKM matrix elements, parameterised in this case by λ. Equation (4) is correct up to $\text{O}(\lambda^4)$.

The CKM matrix affects the weak interactions of quarks. The strong force normally governs quark dynamics, and therefore the elements of the CKM matrix can only be measured in very specific processes. Most often, these processes are the decays of mesons, where decays via the strong or EM forces are forbidden by conservation laws – i.e. for the least massive meson with a given quark content. Some details of how individual CKM matrix elements are measured are given in the lecture notes, but see also the exercises below. Numerically, the absolute values of the CKM matrix elements are measured to be

$$V_{\text{CKM}}^{\text{meas.}} = \begin{pmatrix} 0.97425 \pm 0.00022 & 0.2252 \pm 0.0009 & (4.15 \pm 0.49) \times 10^{-3} \\ 0.230 \pm 0.011 & 1.006 \pm 0.023 & (40.9 \pm 1.1) \times 10^{-3} \\ (8.4 \pm 0.6) \times 10^{-3} & (42.9 \pm 2.6) \times 10^{-3} & 0.89 \pm 0.07 \end{pmatrix},$$
$$(5)$$

and the best-fit values for the Wolfenstein parameters are:[3]

$$\lambda = 0.22535 \pm 0.00065, \qquad\qquad A = 0.811^{+0.022}_{-0.012},$$
$$\bar{\rho} = 0.131^{+0.026}_{-0.013}, \qquad\qquad \bar{\eta} = 0.345^{+0.013}_{-0.014}. \qquad (6)$$

---

[3] $\bar{\rho}$ and $\bar{\eta}$ are defined to take into account higher order corrections in λ.

It should be noted that the matrix in Equation (5) is nearly diagonal – in particular, the elements in the third row and column are extremely small, except for V_{tb}. This latter observation explains why weakly-decaying B hadrons have relatively long lifetimes, $\mathcal{O}(\mathrm{ps})$, compared to what would be expected from phase space considerations alone.

Exercise: Draw Feynman diagrams for the processes below. In each case, work out which CKM element(s) could be constrained by measurements of the process.

- $\pi^+ \to \pi^0 e^+ \nu_e$;
- $K^+ \to \mu^+ \nu_\mu$;
- $\bar{K}^0 \to \pi^+ \pi^-$;
- $K^0 \to \pi^- e^+ \nu_e$;
- $\nu_\mu d \to \mu^- c$ followed by $c \to d \mu^+ \nu_\mu$;
- $B^+ \to D^+ X$ (what could X be?);
- $B^+ \to K^+ \gamma$ (see Figure 6 for inspiration);
- $B_s \to \mu^+ \mu^-$;
- $t \to W^+ b$.

2 The unitarity triangle

Unitarity demands that the rows and columns of the CKM matrix are orthogonal to each other, i.e. they satisfy the following constraints:

$$V_{ud}V_{us}^* + V_{cd}V_{cs}^* + V_{td}V_{ts}^* = 0, \tag{7}$$

$$V_{ud}V_{ub}^* + V_{cd}V_{cb}^* + V_{td}V_{tb}^* = 0, \tag{8}$$

$$V_{us}V_{ub}^* + V_{cs}V_{cb}^* + V_{ts}V_{tb}^* = 0. \tag{9}$$

$$V_{ud}V_{cd}^* + V_{us}V_{cs}^* + V_{ub}V_{cb}^* = 0, \tag{10}$$

$$V_{ud}V_{td}^* + V_{us}V_{ts}^* + V_{ub}V_{tb}^* = 0, \tag{11}$$

$$V_{cd}V_{td}^* + V_{cs}V_{ts}^* + V_{cb}V_{tb}^* = 0, \tag{12}$$

Plotted in an Argand diagram, the three terms in each sum form the sides of a triangle. It can be demonstrated that the areas of these triangles are equal, and they are related to the size of the complex phase, i.e. to the amount of CP violation in weak interactions. It is therefore interesting to measure the sides and angles of these triangles, to test if δ (Equation (4)) is the only source of CP violation in the weak interaction. Four of the six triangles are, however, extremely elongated and difficult to measure. For example, in Equation (9), the magnitudes of the last two terms are $\sim A\lambda^2$, while the first term is $\sim A\lambda^4$, or only about 5% of the size of the other two terms. This makes it difficult to differentiate between a triangle and a straight line in these cases.
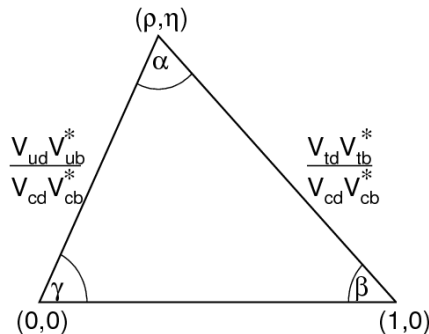
Figure 1: Definition of the sides and angles of the unitarity triangle.

Exercise: Check the sizes of all the elements in Equations (7) to (12).

The remaining two triangles, from Equations (8) and (11), have sides all of a similar length $\sim A\lambda^3$. However, every term in Equation (11) involves a top quark coupling. As these are less well-known experimentally, "the" unitarity triangle is usually understood to correspond to Equation (8).

The unitarity triangle is shown in Figure 1, where the terms in Equation (8) have been normalised by $V_{cd}V_{cb}^*$, which has the smallest overall uncertainty of the three terms (see Equation (5)). Experimental measurements of the three angles and two non-trivial sides can be used to over-constrain the three free parameters of the triangle, and its closure is an important test of the SM. An overview of the current constraints is shown in Figure 2. With two corners of the triangle fixed, all of the constraints can be expressed in terms of the location of the third point. The six constraints (three angles, two sides and one product of real and imaginary components) are all in agreement at the 95% confidence level, supporting the SM hypothesis of flavour mixing via V_{CKM}.

Many of the measurements that contribute to Figure 2 involve the phenomenon of oscillation. It is on this that we now focus, with particular emphasis on CP violation.

3 Oscillations

Flavour oscillations can arise in electrically neutral, weakly decaying mesons because the conservation laws that apply to the strong and weak nuclear forces are different. The strong force conserved flavour, and therefore must produce a meson with a specific flavour eigenstate, for example $K^0 = d\bar{s}$. The weak force does not conserve flavour, but does very nearly conserve CP. Therefore, where possible, the weak decay of mesons proceeds via CP eigenstates. In the case of the neutral mesons, the antiparticle (e.g. $\bar{K}^0 = s\bar{d}$ in this example) is related to the particle by a CP transformation, and so
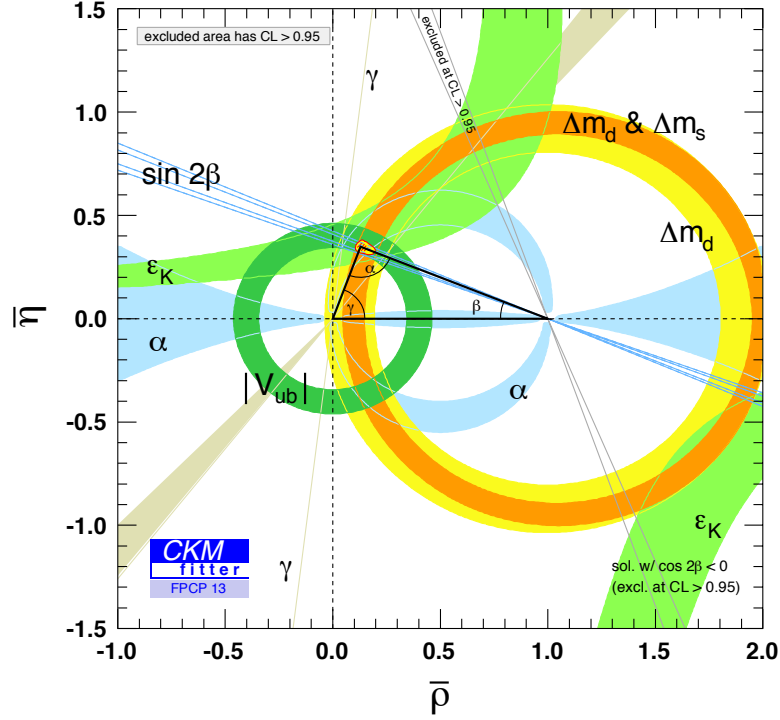
Figure 2: Constraints on the unitarity triangle, expressed as 95% CL uncertainty bands on the position of the upper point of the triangle. The best-fit region is shaded in yellow.

we can easily identify the CP eigenstates of the system:

$$
\begin{aligned}
|K_+^0\rangle &= \frac{1}{\sqrt{2}} \left(|K^0\rangle + |\bar{K}^0\rangle \right), \\
|K_-^0\rangle &= \frac{1}{\sqrt{2}} \left(|K^0\rangle - |\bar{K}^0\rangle \right).
\end{aligned}
\tag{13}
$$

Apart from very small corrections (see Section 4), these can be identified with the weak eigenstates. Each state has its own mass, dependent on the mixing process, and lifetime, dependent on the available decay channels for
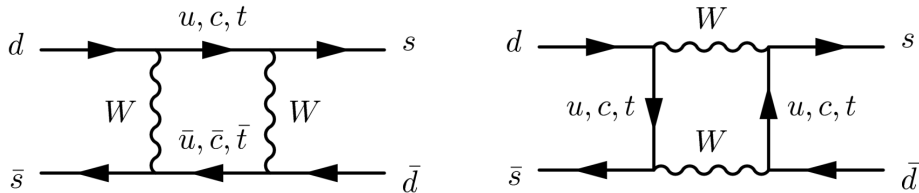

Figure 3: The two leading diagrams for $K^0 - \bar{K}^0$ oscillations.

each meson. Similar expressions hold for the $D^0(c\bar{u})$, $B^0(d\bar{b})$ and $B_s^0(s\bar{b})$ mesons, but we will primarily use the K^0 as an example.

The physical mechanism of flavour oscillation is a second-order weak interaction. The main diagrams contributing to kaon mixing are shown in Figure 3. In principle, all of the up-type quarks contribute inside each loop, although for the reasons explained in the lecture notes the charm quark is the most important in this case.[4] The oscillation rate is in principle calculable, therefore measurements of it can help constrain various CKM matrix parameters and combinations of them (e.g. the band marked "Δm_d & Δm_s" in Figure 2). As the process is highly suppressed, it is also a powerful test of (non-SM) flavour-changing neutral currents.

As an aside, the difference between the CP-even and CP-odd eigenstates is particularly extreme in the kaon system. The CP-even state has two-pion decay channels ($\pi^+\pi^-$ and $\pi^0\pi^0$) available to it; these are forbidden to a CP-odd state by Bose-Einstein statistics. The decay of the CP-odd state to three pions ($\pi^+\pi^-\pi^0$ and $\pi^0\pi^0\pi^0$) is strongly phase-space suppressed as the mass difference between initial and final states is only about 70 MeV.[5] As a result, the lifetimes of the two states differ by three orders of magnitude, leading to the labels of "short" (K_S^0, $\tau \sim 10^{-10}$ s) and "long" (K_L^0, $\tau \sim 10^{-7}$ s) to describe the two physical states.

As the name implies, flavour oscillations have a time-dependence that can be measured by detectors with sufficient resolution.[6] Suppose that we consider the state $|\psi(t)\rangle$ of a kaon that is a pure K^0 state at the point of production. That is:

$$|\psi(0)\rangle = |K^0\rangle = \frac{1}{\sqrt{2}}\left(|K_S^0\rangle + |K_L^0\rangle\right). \tag{14}$$

The K_S^0 and K_L^0 states propagate independently, with their own masses and lifetimes. Using this fact, we can express the state at time t in terms of CP and quark flavour eigenstates:

$$\begin{aligned}
|\psi(t)\rangle &= \frac{1}{\sqrt{2}}\left(e^{\left(im_S - \frac{1}{2\tau_S}\right)t}|K_S^0\rangle + e^{\left(im_L - \frac{1}{2\tau_L}\right)t}|K_L^0\rangle\right) \\
&= \frac{1}{2}\left\{\left(e^{\left(im_S - \frac{1}{2\tau_S}\right)t} + e^{\left(im_L - \frac{1}{2\tau_L}\right)t}\right)|K^0\rangle \right. \\
&\quad \left. + \left(e^{\left(im_S - \frac{1}{2\tau_S}\right)t} - e^{\left(im_L - \frac{1}{2\tau_L}\right)t}\right)|\bar{K}^0\rangle\right\}. \tag{15}
\end{aligned}$$

---

[4] This is very different from B^0 and B_s^0 mixing, where the top quark is most important, making these oscillations essential for measurements of V_{td} and V_{ts}.

[5] In fact, it is so suppressed that the semileptonic decays $K_L^0 \to \pi^\pm \ell^\mp \nu$ become dominant.

[6] Here, we mean spatial resolution, as the displacement of the meson's decay from its point of production can be used to infer its proper lifetime, if its momentum is known.
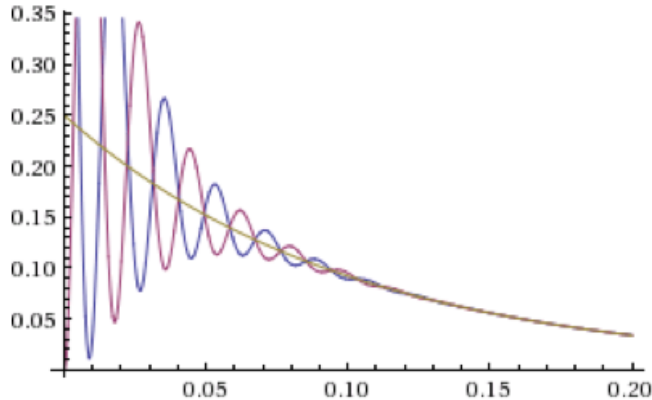
Figure 4: Illustration of the interference between meson and anti-meson states when $\tau_L \gg \tau_S$. Unphysical parameter values are used, to emphasise the oscillations. The blue line represents Equation (16) and the red shows Equation (17), while the yellow line shows $\frac{1}{4}e^{-t/\tau_L}$.

Using Equation (15), we can calculate the probability of finding a K^0 or a $\bar{K}^0$ as a function of time:

$$|\langle K^0|\psi(t)\rangle|^2 = \frac{1}{4}\left[e^{-t/\tau_S} + e^{-t/\tau_L} + 2e^{-t\left(\frac{1}{2\tau_S}+\frac{1}{2\tau_L}\right)}\cos\Delta mt\right], \qquad (16)$$

$$|\langle \bar{K}^0|\psi(t)\rangle|^2 = \frac{1}{4}\left[e^{-t/\tau_S} + e^{-t/\tau_L} - 2e^{-t\left(\frac{1}{2\tau_S}+\frac{1}{2\tau_L}\right)}\cos\Delta mt\right]. \qquad (17)$$

Exercise: Derive these two expressions from Equation (15).

The final term of each line is an interference term, which depends on the mass difference Δm between K^0_S and K^0_L. If $\tau_S \ll \tau_L$, the oscillations decay with a lifetime of $\sim 2\tau_S$. The general form of this interference is shown in Figure 4, although the details depend strongly on the two lifetimes and Δm. In this case, the parameters have been chosen to highlight the decay of the oscillations. In the physical kaon system, Δm and $1/\tau_S$ are of the same order of magnitude, so typically only ~ 1 oscillation can occur before the K^0_S decays away. In the D^0 system, the oscillation time is much longer than the mesons' lifetimes, making its observation very challenging, while in the B^0 and B^0_s systems, all of the oscillation times and lifetimes are $\mathcal{O}(10^{-12})$ s.

4 CP violation in neutral meson oscillations

Figure 5 shows the measured rate of $K^0 \to \pi\pi$ decays in the CPLEAR experiment, as a function of the proper decay time τ. This is proportional to the probability of finding the kaon in the CP-even eigenstate K^0_+. Up to $\tau \sim 12\tau_S$, this falls nearly exponentially (with time constant τ_S), modified
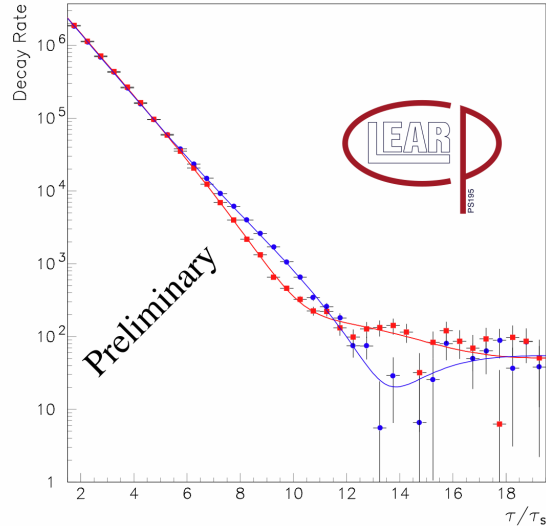
Figure 5: The rate of $K \to \pi\pi$ decays as a function of proper time divided by τ_S. The rate is shown separately for kaons that are initially K^0 (red squares) and $\bar{K}^0$ (blue circles), tagged by the charge of a $K^\pm$ produced in association with the neutral kaon. Note the interference between K_S^0 and K_L^0 states for $6 \lesssim \tau/\tau_S \lesssim 17$, not to be confused with the oscillations shown in Figure 4.

by some interference between the K_S^0 and K_L^0 states (not shown in Equation (15). However, at larger times, the rate flattens out to a nearly constant value, long after the K_S^0 component has decayed away. This indicates that the $K_L^0 \to \pi\pi$ decay is occurring, consequently that the weak interaction does not perfectly conserve CP in this decay.[7]

The dominant CP-violating effect in this case is *indirect* CP violation. This arises because the K_S^0 and K_L^0 particles do not correspond exactly to the CP eigenstates $K_\pm^0$ from Equation (13). Instead, the physical states have small admixtures of the "wrong" CP eigenstate:

$$|K_S^0\rangle = \frac{1}{\sqrt{1+\epsilon^2}} \left(|K_+^0\rangle + \epsilon |K_-^0\rangle \right),$$
$$|K_L^0\rangle = \frac{1}{\sqrt{1+\epsilon^2}} \left(|K_-^0\rangle - \epsilon |K_+^0\rangle \right). \tag{18}$$

Via the CPT theorem, the cause of this can be understood as a difference between the amplitudes for $K^0 \to \bar{K}^0$ and $\bar{K}^0 \to K^0$ oscillations. The $K_L^0 \to \pi\pi$ decay itself proceeds via the K_+^0 component of the K_L^0, and conserves

---

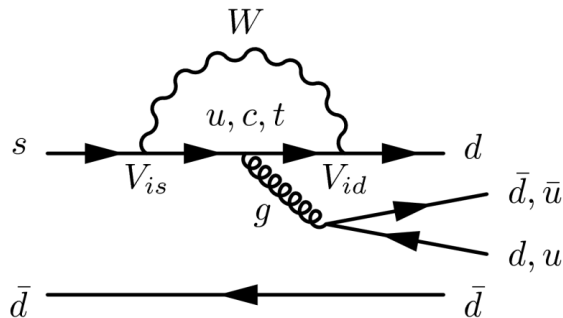[7]Cronin and Fitch were awarded the Nobel prize in 1980 for this observation.

Figure 6: Example of a penguin diagram, responsible for direct CP violation in kaon decays.

CP. The observed CP violation is independent of the decay channel, as it depends only on the size of ϵ, measured to be $(2.228 \pm 0.011) \times 10^{-3}$.

In contrast, *direct* CP violation is a property of the decay process itself. Direct CP violation is possible in certain Feynman diagrams, such as the $\bar{K}^0 \to \pi\pi$ decay illustrated in Figure 6. For historical reasons, this is called a *penguin* diagram, and in this case it competes with direct $s \to uW^{-*} \to ud\bar{u}$ decays that lead to the same final state. To see why this diagram can violate CP, consider just the diagram mediated by a charm quark. The $\bar{K}^0 \to \pi\pi$ amplitude is in this case proportional to $V_{cs}V_{cd}$. The decay $K^0 \to \pi\pi$ is obtained from this by a CP transformation, and the amplitude must be unchanged if the interaction conserved CP. However, the vertex term in this case is proportional to $V_{cs}^* V_{cd}^*$, and may have a non-zero complex phase with respect to the $\bar{K}^0 \to \pi\pi$ decay. The contributions from the other up-type quarks will add with different phases, resulting in a different decay rate for the two states in this channel.

Unlike indirect CP violation, the amplitude for direct CP violating decays depends on the decay channel. For example, the rates for $K_{\mathrm{L}}^0 \to \pi^+\pi^-$ and $K_{\mathrm{L}}^0 \to \pi^0\pi^0$ can be measured separately, and compared to the equivalent K_{S}^0 decays to remove uncertainties in the non-perturbative corrections to the amplitudes. The direct CP violation in these decays is quantified by a parameter ϵ' that depends on the ratio of the two K_{L}^0 decay amplitudes. The system is measured to have a small, but non-zero, direct CP violation:

$$\mathrm{Re}\left(\frac{\epsilon'}{\epsilon}\right) \approx \frac{\epsilon'}{\epsilon} = (1.66 \pm 0.23) \times 10^{-3}, \tag{19}$$

thus confirming that both mechanisms contribute in this decay.

9